BJ www.biochemj.org

Biochem. J. (2012) **443**, 515–523 (Printed in Great Britain) doi:10.1042/BJ20111871

SUPPLEMENTARY ONLINE DATA

Calcium/calmodulin inhibition of the *Arabidopsis* BRASSINOSTEROID-INSENSITIVE 1 receptor kinase provides a possible link between calcium and brassinosteroid signalling

Man-Ho OH*, Hyoung Seok KIM*, Xia WU*, Steven D. CLOUSE†, Raymond E. ZIELINSKI* and Steven C. HUBER*‡[1]

*Department of Plant Biology, University of Illinois, Urbana, IL 61801, U.S.A., †Department of Horticultural Science, NC State University, Raleigh, NC 27695, U.S.A., and ‡U.S. Department of Agriculture, Agricultural Research Service, Urbana, IL 61801, U.S.A.

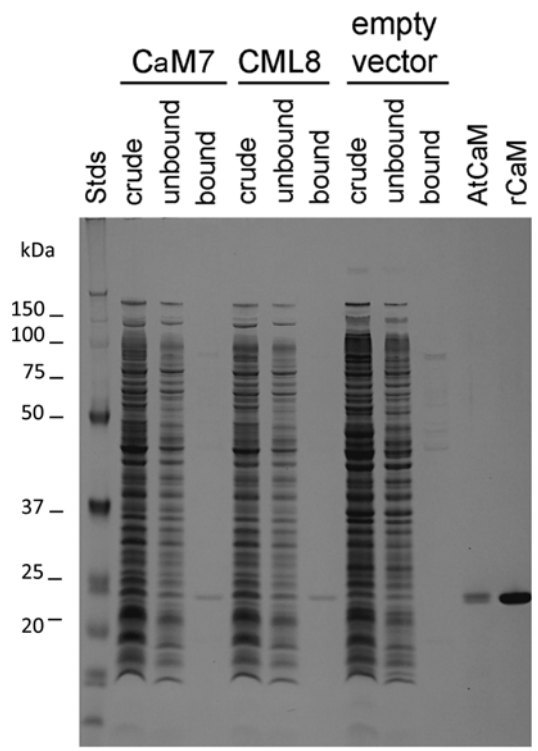

Figure S1 Constitutive expression of CaM in *E. coli* driven by pRZ528 (CaM7) and 529 (CML8)

Total soluble proteins were extracted from late-exponential-phase bacteria, clarified by centrifugation and subjected to Ca^{2+}-dependent HIC (hydrophobic interaction chromatography) on phenyl-Sepharose. Samples of the crude extract, the fraction that did not bind to phenyl-Sepharose (unbound), and the fraction that eluted from the resin in the presence of EDTA (bound) were separated by SDS/PAGE and stained with Coomassie Brilliant Blue. Purified AtCaM and recombinant CaM (rCaM) were fractionated in parallel as positive controls together with molecular mass standards (Stds, sizes given in kDa).

```
..815     REMRKR RRKKEAELEM YAEGHGNSGD RTANNTNWKL TGVKEALSIN
.....      000000 0000000000 0000000000 0000001112 3333333333

..861 LAAFEKPLRK LTFADLLQAT NGFHNDSLIG SGGFGDVYKA ILKDGSAVAI
..... 3333332211 0000000000 0000000000 0000000000 0000000000

..911 KKLIHVSGQG DREFMAEMET IGKIKHRNLV PLLGYCKVGD ERLLVYEFMK
..... 0000000000 0000000000 0000000000 0000000000 0000000000

..961 YGSLEDVLHD PKKAGVKLNW STRRKIAIGS ARGLAFLHHN CSPHIIHRDM
..... 0000000112 2234456789 9999999987 7765443211 0000000000

.1011 KSSNVLLDEN LEARVSDFGM ARLMSAMDTH LSVSTLAGTP GYVPPEYYQS
..... 0000000000 0000000000 0000000000 0000000000 0000000000

.1061 FRCSTKGDVY SYGVVLLELL TGKRPTDSPD FGDNNLVGWV KQHAKLRISD
..... 0000011111 1111111111 1111100000 0000000000 0000000000

.1111 VFDPELMKED PALEIELLQH LKVAVACLDD RAWRRPTMVQ VMAMFKEIQA
..... 0000000000 0000000000 0000000000 0000000000 0000000000

.1161 GSGIDSQSTI RSIEDGGFST IEMVDMSIKE VPEGKL
..... 0000000000 0000000000 0000000000 000000
```

Figure S2 BRI1 cytoplasmic domain sequence showing predicted probabilities of CaM binding

The numbers below the sequence indicate the probability of CaM binding (http://calcium.uhnres.utoronto.ca/ctdb/ctdb/home.html) with 9 being the highest score. The kinase domain of BRI1 is shown in red, and the sequences used to generate the W980 and W1099 peptides are underlined.

[1] To whom correspondence should be addressed (email schuber1@illinois.edu).

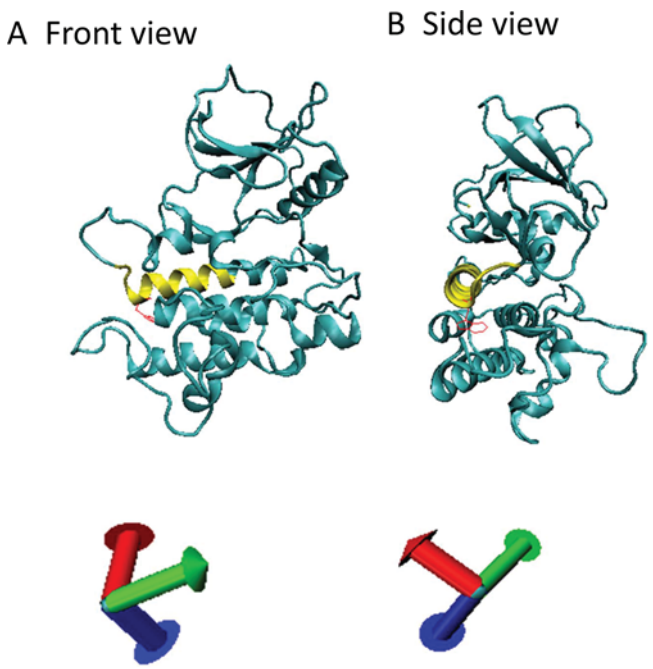

Figure S3 Model of the BRI1 kinase domain structure

The BRI1 kinase domain was modelled as described in the Experimental section of the main text. The location of the predicted CaM-binding site (Leu^{978}–Arg^{992}) is shown in yellow and the Try^{980} side chain is shown in red. (**A**) Front view. (**B**) Side view.

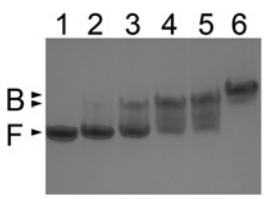

Figure S4 Gel mobility-shift analysis of AtCaM6 interaction with W980 peptide

AtCaM6 (300 pmol/reaction) was incubated with 0 (lane 1), 150 (lane 2), 300 (lane 3), 600 (lane 4) or 1200 (lane 5) pmol of W980 peptide or 300 pmol of a CaM-binding peptide from CaMKII (lane 6) then fractionated in a non-denaturing gel containing Ca^{2+}. Coomassie Brilliant Blue staining revealed the migration of free (F) and peptide-bound (B) AtCaM6. The larger size of the CaMKII peptide resulted in a slower mobility of the peptide–AtCaM6 complex compared with the W980 peptide complex.

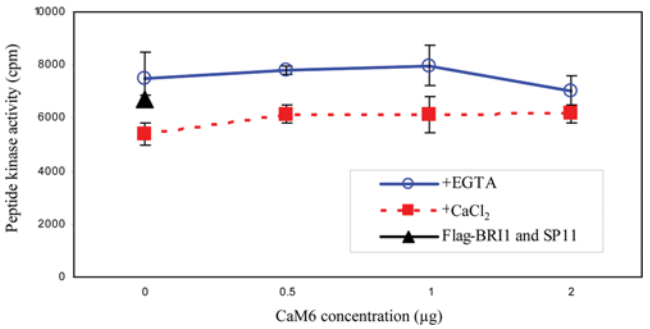

Figure S5 AtCaM6 has no effect on BRI1 peptide kinase activity *in vitro*

BRI1 peptide kinase activity was assayed using [^{32}P]ATP and the SP11 synthetic peptide as substrate as described in [1] with the addition of 0.1 mM $CaCl_2$ or 1 mM EGTA as indicated. Each reaction contained 0.5 μg of FLAG–BRI1 protein, and reactions were run for 5 min.

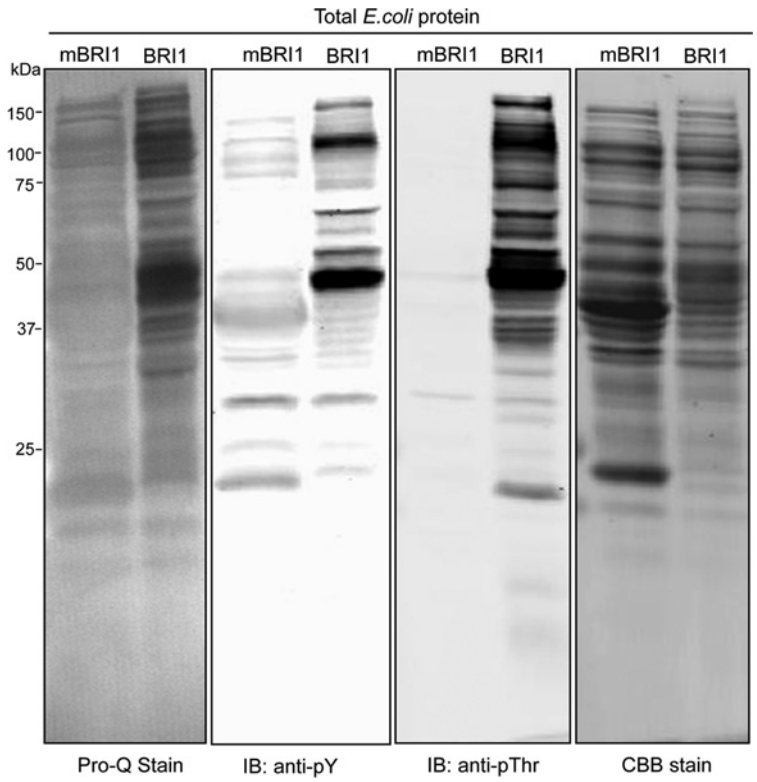

Figure S6 Kinase-inactive mBRI1 does not transphosphorylate *E. coli* proteins

BRI1 or the kinase-inactive mBRI1 (mutant BRI1) were expressed in *E. coli* and following purification of the FLAG-tagged proteins, the remaining *E. coli* proteins were analysed for phosphorylation by Pro-Q Diamond phosphoprotein staining or immunoblotting (IB) with generic anti-phosphotyrosine or anti-phosphothreonine antibodies. Molecular masses are indicated in kDa.

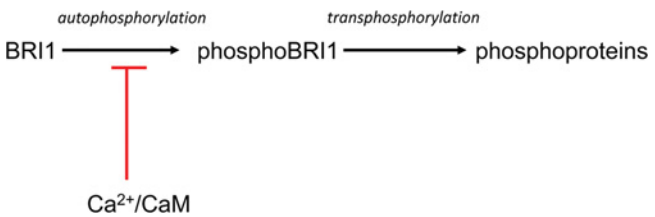

Figure S7 Working model for effects of Ca^{2+}/CaM on BRI1

We propose that Ca^{2+}/CaM inhibits BRI1 autophosphorylation, which then affects transphosphorylation activity. Thus certain CaM and CML isoforms inhibit BRI1 autophosphorylation when co-expressed in *E. coli* and, as a result, also inhibit the transphosphorylation of *E. coli* proteins. This provides a plausible explanation for why Ca^{2+}/CaM inhibits transphosphorylation in the *in situ* system, but does not affect transphosphorylation activity *in vitro* (peptide kinase activity). The model predicts that Ca^{2+} signalling during early stages of BRI1 activation will attenuate downstream signal transduction.

Table S1 Identification of BRI1-mediated phosphorylation sites on *E. coli* proteins

LC–MS/MS results identifying BRI1-mediated phosphorylation sites on *E. coli* proteins, obtained by enrichment of phosphopeptides using TiO_2, Fe^{3+}-IMAC (IMAC) or processing bodies (P-bodies) as indicated. M_r(expt), expected molecular mass; M_r(calc), calculated molecular mass; MC, the number of missed cleavages; Score, Mascot score, which is a probability-based implementation of the Mowse algorithm. The total score is the absolute probability that the observed match is a random event and is calculated as $-10\cdot\log_{10}(P)$, where P is the absolute probability. Expect, expectation value, which is directly equivalent to the *E*-value in a BLAST search result. The lower the expectation value, the more significant the score.

Source	Site	Name	M_r(expt)	M_r(calc)	Delta	MC	Score	Expect	Peptide
TiO_2	Thr^{4}	hupA	1581.3848	1581.7837	−0.3989	1	101	1.40×10^{-8}	-.MNK**pT**QLIDVIAEK.A
IMAC	Thr^{19}	hupA	1054.2634	1054.506	−0.2425	1	30	0.018	K.AELSK**pT**QAK.A
IMAC	Ser^{17}/Thr^{19}	hupA	1134.2084	1134.4723	−0.2638	1	45	0.00029	K.AEL**pS**K**pT**QAK.A
TiO_2	Ser^{27}/Thr^{33}	hupA	1676.3594	1676.7674	−0.4080	0	53	2.40×10^{-5}	K.AALE**pS**TLAAI**pT**ESLK.E
TiO_2	Thr^{28}/Thr^{33}	hupA	1676.3608	1676.7674	−0.4066	0	57	8.90×10^{-6}	K.AALES**pT**LAAI**pT**ESLK.E
TiO_2	Ser^{81}	hupA	1323.3224	1323.6588	−0.3363	0	79	2.00×10^{-7}	K.IAAANVPAFV**pS**GK.A
TiO_2	Ser^{4}	hupB	1155.2196	1155.5359	−0.3162	1	40	0.016	-.MNK**pS**QLIDK.I
P-bodies	Ser^{4}	hupB	1024.2108	1024.4954	−0.2845	1	43	0.0008	M.NK**pS**QLIDK.I
TiO_2	Thr^{65}/Thr^{70}	hupB	1600.3228	1600.7263	−0.4034	1	109	7.00×10^{-10}	R.NPQ**pT**GKEI**pT**IAAAK.V
TiO_2	Ser^{21}	groS	1281.3088	1281.6330	−0.3241	0	65	1.80×10^{5}	K.**pS**AGGIVLTGSAAAK.S
TiO_2	Thr^{28}	groS	1281.3080	1281.6330	−0.3249	0	43	0.00041	K.SAGGIVL**pT**GSAAAK.S
TiO_2	Ser^{21}/Thr^{28}	groS	1361.2596	1361.5993	−0.3396	0	89	3.70×10^{-8}	K.**pS**AGGIVL**pT**GSAAAK.S
TiO_2	Ser^{21}/Ser^{30}	groS	1361.2416	1361.5993	−0.3576	0	74	1.70×10^{-6}	K.**pS**AGGIVLTG**pS**AAAK.S
TiO_2	Ser^{28}	lacI	1218.2710	1218.5758	−0.3047	0	47	8.30×10^{5}	R.VVNQA**pS**HVSAK.T
TiO_2	Ser^{28}/Ser^{31}	lacI	1298.1776	1298.5421	−0.3645	0	74	4.20×10^{-7}	R.VVNQA**pS**HV**pS**AK.T
TiO_2	Ser^{28}/Thr^{34}	lacI	1555.2901	1555.6909	−0.4008	1	75	4.40×10^{-7}	R.VVNQA**pS**HVSAK**pT**R.E
TiO_2	Ser^{31}/Thr^{34}	lacI	1555.3120	1555.6909	−0.3789	1	78	7.70×10^{-7}	R.VVNQASHV**pS**AK**pT**R.E
TiO_2	$Ser^{28}/Ser^{31}/Thr^{34}$	lacI	1635.2568	1635.6572	−0.4004	1	96	6.40×10^{-9}	R.VVNQA**pS**HV**pS**AK**pT**R.E
TiO_2	Ser^{93}/Ser^{97}	lacI	1719.3072	1719.7304	−0.4231	0	49	0.00021	R.ADQLGA**pS**VVV**pS**MVER.S
TiO_2	Thr^{334}	lacI	1436.3126	1436.6661	−0.3534	0	89	7.90×10^{-8}	K.TTLAPN**pT**QTASPR.A
TiO_2	Thr^{328}/Thr^{329}	lacI	1880.3242	1880.7948	−0.4705	2	74	2.20×10^{-7}	K.RK**pT**pTLAPN**pT**QTASPR.A
TiO_2	Ser^{345}	lacI	1267.2794	1267.5995	−0.3201	0	78	8.20×10^{-7}	R.ALAD**pS**LMQLAR.Q
TiO_2	Thr^{144}	rpsA	991.1918	991.4376	−0.2457	0	24	0.026	R.D**pT**LHLEGK.E
TiO_2	Ser^{169}	rpsA	866.1780	866.4011	−0.2231	0	35	0.0096	R.NNVVV**pS**R.R
TiO_2	Thr^{455}/Thr^{459}	rpsA	1488.3286	1488.6990	−0.3704	1	98	4.00×10^{-9}	K.GAIV**pT**GKV**pT**AVDAK.G
P-bodies	Thr^{2}/Ser^{4}	rpsA	1818.2380	1818.7188	−0.4807	0	45	1.10×10^{-4}	-.M**pT**E**pS**FAQLFEESLK.E
TiO_2	Ser^{73}	rpsI	1122.2354	1122.5183	−0.2828	0	106	6.90×10^{-9}	K.GGGI**pS**GQAGAIR.H
IMAC	Ser^{128}	rpsI	997.2474	997.4858	−0.2384	1	19	0.15	R.RRPQF**pS**K.R
TiO_2	Thr^{20}/Ser^{21}	rpsM	1587.3568	1587.7463	−0.3894	0	95	8.00×10^{-9}	K.HAVIAL**pT**p**S**IYGVGK.T
TiO_2	Ser^{74}/Ser^{76}	rpsM	1278.2396	1278.5556	−0.316	2	46	0.0013	R.REI**pS**M**pS**IKR.L
TiO_2	Ser^{22}/Thr^{24}	rpsE	1486.3968	1486.7673	−0.3705	2	42	0.00069	K.LIAVNRV**pS**K**pT**VK.G
IMAC	Thr^{20}	rpsB	1188.2416	1188.5190	−0.2773	0	67	9.70×10^{-6}	K.AGVHFGHQ**pT**R.Y
TiO_2	Ser^{95}/Thr^{96}	rpsK	1285.1976	1285.5217	−0.3241	1	36	0.0043	K.GPGPGRE**pS**p**T**IR.A
P-bodies	Thr^{3}/Thr^{10}	rplM	1695.3088	1695.782	−0.4732	2	58	2.50×10^{-5}	-.MK**pT**FTAKPE**pT**VKR.D
TiO_2	$Thr^{3}/Thr^{5}/Thr^{10}$	rplM	1775.2999	1775.7483	−0.4485	2	79	3.40×10^{-7}	-.MK**pT**F**pT**AKPE**pT**VKR.D
TiO_2	Thr^{5}/Ser^{12}	rplO	1403.2528	1403.6098	−0.3570	1	43	0.00054	R.LN**pT**LSPAEG**pS**KK.A
TiO_2	Ser^{25}/Thr^{30}	rplO	1218.2586	1218.5159	−0.2573	1	5	1.1	R.GIG**pS**GLGK**pT**GGR.G
TiO_2	Ser^{73}	rplE	687.1339	687.2993	−0.1654	0	33	0.046	K.**pS**VAGFK.I
TiO_2	Thr^{63}/Thr^{69}	rplA	1224.2044	1224.5054	−0.3009	0	25	0.0069	R.GA**pT**VLPHG**pT**GR.S
TiO_2	Thr^{51}/Thr^{52}	rplC	1175.2374	1175.5352	−0.2978	1	20	0.013	R.AIQV**pT**p**T**GAKK.A
IMAC	Ser^{19}/Thr^{25}	rpmB	1156.2116	1156.4791	−0.2674	1	64	3.90×10^{-5}	R.**pS**HALNA**pT**KR.R
IMAC	$Thr^{14}/Ser^{19}/Thr^{25}$	rpmB	2130.4324	2130.9238	−0.4914	2	62	2.00×10^{-6}	K.RPV**pT**GNNR**pS**HALNA**pT**KR.R
IMAC	$Ser^{30}/Thr^{37}/Thr^{39}$	rplV	1960.4137	1960.8713	−0.4576	2	51	0.00023	K.KV**pS**QALDIL**pT**Y**pT**NKK.A
TiO_2	Thr^{60}/Thr^{65}	dnaK	1703.3538	1703.7685	−0.4146	0	38	0.00088	R.QAV**pT**NPQN**pT**LFAIK.R
TiO_2	Ser^{453}	dnaK	1677.3844	1677.7876	−0.4031	0	88	1.50×10^{-7}	K.**pS**LGQFNLDGINPAPR.G
TiO_2	Ser^{505}	dnaK	1369.2368	1369.5762	−0.3394	0	67	1.10×10^{-6}	K.AS**pS**GLNEDEIQK.M
TiO_2	Ser^{201}	gapA	1480.3204	1480.6923	−0.3718	0	65	4.30×10^{-6}	R.GA**pS**QNIIPSSTGAAK.A
TiO_2	Ser^{201}/Ser^{207}	gapA	1560.2696	1560.6586	−0.3889	0	39	0.00055	R.GA**pS**QNIIP**pS**STGAAK.A
P-bodies	Ser^{201}/Thr^{209}	gapA	1560.2372	1560.6586	−0.4213	0	38	0.0011	R.GA**pS**QNIIPSS**pT**GAAK.A
TiO_2	Ser^{239}/Thr^{244}	gapA	1654.3610	1654.7733	−0.4122	0	119	1.20×10^{-10}	R.VPTPNV**pS**VVDL**pT**VR.L
IMAC	Ser^{190}	gapA	1376.2531	1376.5874	−0.3344	1	77	2.80×10^{-7}	K.TVDGP**pS**HKDWR.G
TiO_2	Thr^{544}/Thr^{552}	rpoD	1454.2760	1454.6320	−0.3559	0	62	2.10×10^{-6}	R.AA**pT**HDVLAGL**pT**AR.E
TiO_2	Ser^{602}/Ser^{604}	rpoD	1239.2252	1239.5162	−0.2910	1	29	0.0058	R.HP**pS**R**pS**EVLR.S
TiO_2	Thr^{67}/Thr^{74}	ihfA	1570.2908	1570.6793	−0.3885	1	103	5.00×10^{-10}	R.NPK**pT**GEDIPI**pT**AR.R
TiO_2	Thr^{66}	ihfB	1154.2326	1154.5220	−0.2894	1	60	5.60×10^{-5}	K.**pT**GDKVELEGK.Y
TiO_2	Ser^{72}	tig	1212.2142	1212.5210	−0.3067	0	90	2.90×10^{-7}	R.QDVLGDLM**pS**R.N
TiO_2	Ser^{9}	crr	1211.3148	1211.6162	−0.3014	2	65	1.00×10^{-5}	K.LK**pS**LVSDDKK.D
TiO_2	Ser^{9}/Ser^{12}	crr	1291.2638	1291.5826	−0.3187	2	51	0.00038	K.LK**pS**LV**pS**DDKK.D
TiO_2	Ser^{2}/Thr^{6}	cspA	1079.1738	1079.4487	−0.2749	1	43	0.0017	M.**pS**GKM**pT**GIVK.W
TiO_2	Thr^{324}/Thr^{327}	ftsZ	1329.2768	1329.6095	−0.3326	0	67	1.60×10^{-6}	K.RPEI**pT**LV**pT**NK.Q
TiO_2	Thr^{71}/Thr^{78}	tatA	1991.2990	1991.7986	−0.4997	2	60	8.70×10^{-5}	K.QAD**pT**NQEQAK**pT**EDAKR.H
TiO_2	Ser^{54}/Thr^{60}	infB	1387.2484	1387.5898	−0.3413	1	54	0.0001	K.N**pS**GPDKL**pT**LQR.K
TiO_2	Ser^{9}/Thr^{14}	accD	1188.2380	1188.5305	−0.2924	1	52	0.00042	R.IK**pS**NITP**pT**R.K

Table S1 Continued

Source	Site	Name	M_r(expt)	M_r(calc)	Delta	MC	Score	Expect	Peptide
TiO_2	Thr^{3}	gatZ	911.2322	911.4663	−0.2341	1	46	0.0025	-.MK**pT**LIAR.H
TiO_2	Ser^{476}	aspA	1106.1322	1106.3917	−0.2595	1	45	0.0017	K.RYTDE**pS**EQ.-
TiO_2	Thr^{626}/Thr^{630}	pnp	1082.1788	1082.4563	−0.2774	1	36	0.0098	R.VY**pT**GKV**pT**R.I
TiO_2	Ser^{3}/Thr^{8}	gatD	1592.2680	1592.6671	−0.3990	1	41	0.00036	-.MK**pS**VVND**pT**DGIVR.V
TiO_2	Thr^{87}/Thr^{97}	sucB	1878.3088	1878.7761	−0.4673	2	40	0.0014	K.E**pT**SAKSEEKAS**pT**PAQR.Q
TiO_2	Ser^{75}	frr	927.1428	927.3773	−0.2344	0	39	0.0078	R.SM**pS**PAVEK.A
TiO_2	Ser^{2}	lipA	1038.2284	1038.4933	−0.2648	0	30	0.019	M.**pS**KPIVMER.G
IMAC	Thr^{6}	yqjD	1316.2666	1316.5874	−0.3208	1	54	5.00×10^{-5}	M.SKEH**pT**TEHLR.A
IMAC	Thr^{7}	yqjD	1316.2684	1316.5874	−0.3190	1	33	0.0047	M.SKEHT**pT**EHLR.A
IMAC	Thr^{6}/Thr^{7}	yqjD	1396.2338	1396.5537	−0.3199	1	67	5.80×10^{-6}	M.SKEH**pTpT**EHLR.A
IMAC	Thr^{17}	espF	921.2758	921.4069	−0.1311	0	29	0.026	R.HI**pT**SAASR.V
IMAC	Thr^{76}	grpE	1238.3146	1238.6020	−0.2873	2	28	0.039	R.RR**pT**ELDIEK.A
IMAC	Thr^{94}	tufA	2736.8350	2737.2639	−0.4289	0	25	0.024	K.NMI**pT**GAAGMDGAILVVAATDGPMPQTR.E
P-bodies	Thr^{176}/Ser^{180}	ahpC	1658.2694	1658.7205	−0.4511	0	35	0.0025	K.EGEA**pT**LAP**pS**LDLVGK.I

REFERENCE

1 Oh, M.-H., Ray, W. K., Huber, S. C., Asara, J. M., Gage, D. A. and Clouse, S. D. (2000) Recombinant brassinosteroid insensitive 1 receptor-like kinase autophosphorylates on serine and threonine residues and phosphorylates a conserved peptide motif *in vitro*. Plant Physiol. **124**, 751–766

Received 19 October 2011/30 January 2012; accepted 7 February 2012
Published as BJ Immediate Publication 7 February 2012, doi:10.1042/BJ20111871